

## Article

# A Giant Slide within the Upper Cretaceous Limestones as an Indicator for Fault Activity Dating and Basin Evolution

Nikolaos Dimopoulos <sup>1</sup>, Elena Zoumpouli <sup>1</sup>, Nicolina Bourli <sup>1</sup>, Penelope Papadopoulou <sup>2</sup>, George Iliopoulos <sup>2</sup> and Avraam Zelilidis <sup>1</sup>

<sup>1</sup> Laboratory of Sedimentology, Department of Geology, University of Patras, 26504, Rion, Greece

<sup>2</sup> Laboratory of Paleontology and Stratigraphy, Department of Geology, University of Patras, 26504, Patras, Greece

\* Correspondence: nikos.dhmopoulos@gmail.com; Tel.: +30 6943769695.

**Abstract:** The studied section, up to 10m thick, with 17 different carbonate beds, showed the interaction between a giant slide and the pre-existing normal faults, during the upper Cretaceous time. There are three major points in the studied section: (1). The presence of two slump horizons, up to 1m thick each, within the stratigraphic column, related with the basin floor instability, due to normal listric faults activity, (2). The presence of many normal, with listric geometry, faults, with an ESE-WNW direction, and mostly west dipping. These faults acted during the sedimentation processes and produced the basin floor inclination for the slumping, when still the sediments were unconsolidated. This tectonic activity seems to terminate in the upper part of the stratigraphic column, (3). After the development of the slumps and the normal faults activity, that produced a displacement up to 30cm, a new event was characterized the region. The completely studied block probably rotated to the west and thus the instability of the sediments produced a giant slide, with up to 7m thick and movement up to 0.9m, cutting the pre-existing normal faults. The knowledge of the regional evolution, with extensional tectonic during Jurassic to early Miocene that was inverted to compressional regime, during middle Miocene, and the presence of a major normal fault along the studied section, with an NNW-SSE direction, introduced that the studied section was situated on the hangingwall of the above fault, during the extensional regime.

**Keywords:** slide; soft-sediment deformation structures; Apulian Platform; Kefalonia Island

**Citation:** Dimopoulos N.; Zoumpouli E.; Bourli N.; Papadopoulou P.; Iliopoulos G.; Zelilidis Z. A giant slide within the upper Cretaceous limestones as an indicator for fault activity dating and basin evolution. *Proceedings* **2022**, *69*, x. <https://doi.org/10.3390/xxxxx>

Academic Editor: Firstname Last-name

Published: date

**Publisher's Note:** MDPI stays neutral with regard to jurisdictional claims in published maps and institutional affiliations.



**Copyright:** © 2022 by the authors. Submitted for possible open access publication under the terms and conditions of the Creative Commons Attribution (CC BY) license (<https://creativecommons.org/licenses/by/4.0/>).

## 1. Introduction

Tectonic intensity greatly affects the development of depositional successions of the area that makes it crucial about the period that took place. Inversion tectonic is characterized as the reverse from subsidence to uplift due to the contraction and subsequent reactivation of previously extensional faults [1–3].

Landslides contribute to dismantle active mountain belts [4,5], and faults control the location and abundance of landslides caused by seismic and meteorological triggers [6,7]. Landscape evolution models predict higher rates of landslide erosion near faults [8,9]. However, empirical evidence of the long-term, regional dependency of landslides on active faults remains scarce [10]. Slump is a type of slide (movement as a mass) that takes place within thick unconsolidated deposits. Slumps involve movement along one or more curved failure surfaces, with downward motion near the top and outward motion toward the bottom. They are typically caused by an excess of water within these materials on a steep slope [11].

The objective of this study is to recognize the generating mechanism of slides and slumps, to understand their relationship with the basin geometry and evolution and to relate them with fault activity and the age of their formation.

## 2. Geological Setting

The Hellenic Fault and Thrust Belt (HFTB) dominates the External Hellenides and is mainly controlled by the collision and the continued convergence of the African and Eurasian plates since the Mesozoic [12].

In Kefalonia Island, the Apulian Platform Margins (APM) were deformed from the compression of the Ionian Thrust producing several small foreland basins. The Paliki Peninsula is at close proximity to the Kefalonia strike-slip fault and exhibits slumped blocks to opposite direction (eastward directed) over younger deposits [13] (Figure 1).

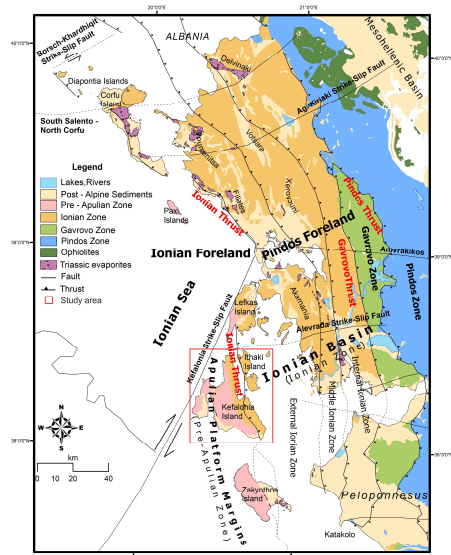


**Figure 1.** Simplified geological map of the Ionian Basin and the Apulian Platform Margins (APM), showing the major structural elements. The studied Kefalonia Island is marked with a red box [14].

The main structural pattern of Kefalonia Island consists of inverse faults and over-thrusts. The over-thrust of Ionian Basin on Pre-Apulian Platform are affected by two thrusts, Atheros and Enos thrusts, causing the contact between different depositional successions [15] (Figure 2).

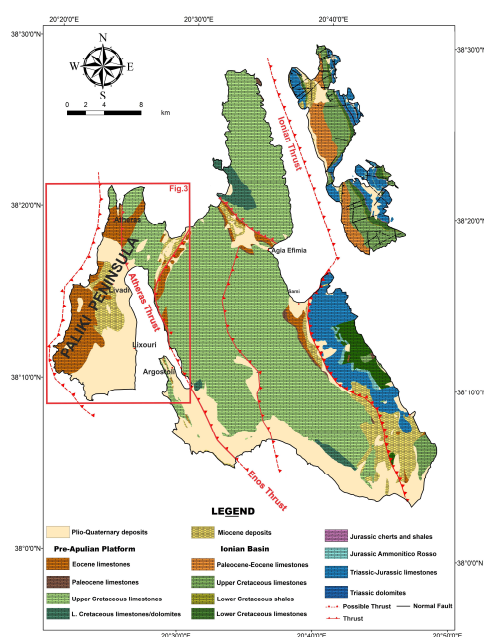


**Figure 2.** The geological map of the Island of Kefalonia. The studied Paliki Peninsula is marked with a red box.

Accordi et al. [15, 16] introduced six (6) different sectors (from I to VI) in the study area of Paliki Peninsula (Figure 3). From sector I up to sector III that located west of the Atheras Thrust, a progressive increase of a hiatus was recognized. A subaerial exposure of the whole area was suggested, that was terminated by the onset of shallow water sedimentation, followed by an increasing deepening. East of the Atheras thrust, in Rahi-Loutsia sector (Sector IV), the restricted inner-ramp facies were missing, whereas the sequence shows a wider textural variability of the middle-outer ramp facies, some in situ, some others resedimented. Sector V in Zola is the tectonic contact between the shallow water succession of sector IV and the toe of slope succession of sector VI hidden by Miocene and Plio-Pleistocene deposits. Finally, east of Enos thrust, the sector VI, with a toe of slope sedimentation, persists throughout the Senonian without significant changes, was recognized.

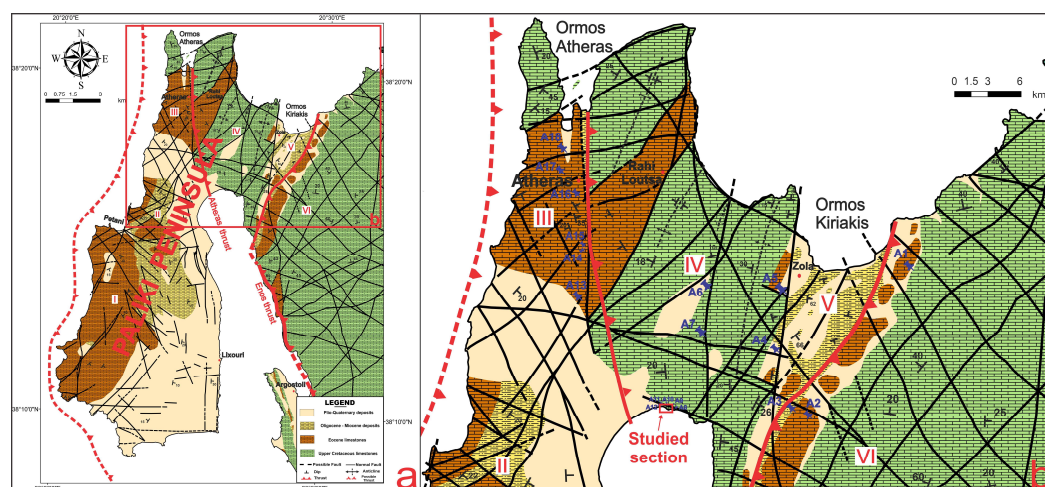


**Figure 3.** (a) The geological map of the studied Paliki Peninsula. Red box shows the studied area; (b) A detailed map showing the studied northern part of the Paliki Peninsula with the location of the selected samples.

In general, they introduced that from west to east, at the lower stratigraphic parts, a sabha and tidal flat environment (Atheras sector III) pass laterally to subtidal protected lagoon (Rahi-Loutsia sector IV) and finally to the toe of slope (Zola sector V). In the upper stratigraphic parts and from west to east a tidal flat–protected lagoon pass from a subtidal protected lagoon to open marine shoal and finally to the toe of slope.

### 3. Material and Methods

The depositional conditions and the age determinations were based on selected samples from the western part of Kefalonia Island, from which thin sections were prepared. Sampling was run in carbonate deposits of different age in the Paliki Peninsula and was organized according to the pre-existing geological map of Kefalonia Island. Eighteen samples in Paliki Peninsula were collected.

The selection of the samples was based on lithology and facies alternations (Figure 3). All samples were cut, and thin sections were prepared for microfacies analysis in order to establish the temporal and spatial changes and the evolution of the respective depositional paleoenvironments in the study area (Figure 3).

Microfacies analysis was used to identify the depositional environments and the dynamic conditions of the carbonate sequence in the northern part of Paliki Peninsula in different positions of the basin. The textural characters of microfacies types were defined according to Dunham’s [17] classification modified by Embry and Klovan, [18] and Flügel [19], and their description includes biogenic and inorganic dominant components of depth and depositional environment [20–22].

#### 4. Depositional Conditions and Age Determination

The microfacies analysis in the studied thin sections (for the location of samples see Figure 3b) showed that we have samples that deposited in deep water conditions in a pelagic environment (FZ3/FZ4) as well as some samples that deposited in a shallower water condition in an open marine-restricted environment (FZ7/FZ8).

Especially, samples A1, A3, A14, A15 and A17 were classified as SMF3, which deposited in a moderately inclined sea floor and basinwards of the steeper slope environment that belong to facies zone FZ4. Samples A13 and A18 samples classified as SMF5 type that belong to facies zone FZ3. Both FZ3 and FZ4 facies zones represent slope depositional environment conditions.

In addition samples A2, A4, A5, A7, A8 were classified as SMF 8-9 type that belong to facies zone FZ7. Although A6 and A16 were classified as SMF 17-18 type that also belong to FZ7 facies zone. There were also same samples (A9, A10, A11, A12) that were classified as SMF 19-20 type and belong to facies zone FZ8. In these samples that represents FZ7 and FZ8 facies zone we have the presence of benthic foraminifera and algae. Both FZ7 and FZ8 facies zones, representing an open marine-restricted environment.

#### 5. Field Work

The studied section along the road from Argostoli to Lixouri and close to the isthmus of Paliki peninsula is 230m length and up to 10m thick, with an overall NW-SE direction with 15°, up to 23° dip (Figure 4). Seventeen (17) different beds were recognized, which some of them present internal differences and could be related with different time of the development. The beds of the studied section present different thicknesses from medium to thick-bedded limestones (0.3 m to 2 m).

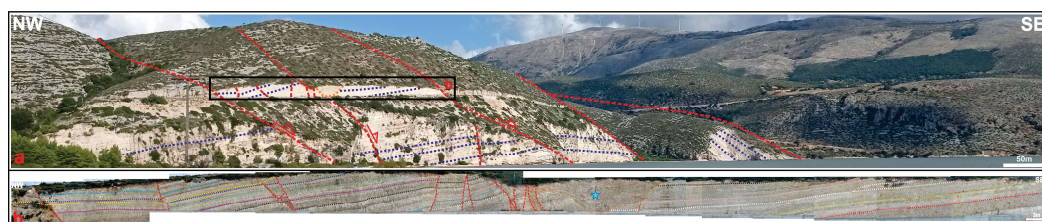


**Figure 4.** Panoramic view of the study area. The red dashed lines show the normal faults that influenced sedimentation processes and the black box shows the studied section.

Two slump horizons, up to 1m thick each, with sharp and erosional contacts, were recognized in the eastern side of the section. Twelve (12) faults were measured in the western part of the section. The above faults have a listric geometry, with an ESE-WNW direction. Most of them dip to the west and some of them show an east dip. The synchronous activity of the above faults produced either a synthetic scale or a horst geometry. A detachment surface of a giant slide, up to 5 m thick, also was recognized in western part of the studied section. Finally, a recent fluvial channel, 20 m wide and 4m thick, with erosional contact, was recognized, that was developed due synthetic and antithetic fault activity.

##### 5a. Slump Horizons

The presence of two slump horizons, horizons two (2) and seven (7), were recognized. Both slumps showed that sourced from the east, as a result of tectonic activity (Figure 5).

The first slump horizon (2) showed an outcrop of 71 m long and 1.8 m thick, with flat base, erosional upper surface (Figure 5a1) and high lateral stable thickness. Over the later five (5) undeformed horizons were developed with flat bases, except this of horizon 3, who rest over the horizon 2 with an erosional contact (Figure 5a2).

The second slump horizon (7) wedged out northwards, showed an outcrop of 88 m along and 1.2 m thick (Figure 5a2), with reduce of its thickness from 1.2 m to 0.3 m (Figure 5a3).

The geometry of these two slumps and the internal clast size introduce that both sourced from south.

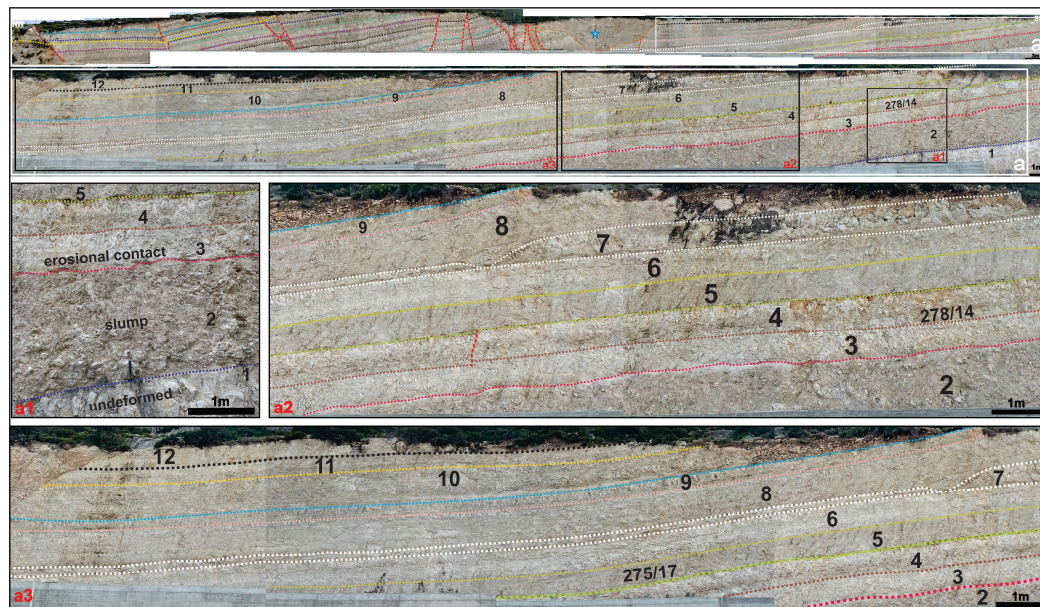


**Figure 5.** On the top the studied section is shown, where with white box the exact location of photograph a is marked; (a1) a slump horizon (horizon 2) between the undeformed horizons (1,3) with an erosional top surface; (a2, a3) Medium interbedded limestones with showing the two slump horizons (2,7) and their lateral extension.

### 5b. Normal with Listric Geometry Faults, Most of Them with an ESE-WNW Direction

In the studied section, twelve (12) normal faults were measured, only in the western part of the section. Most of them showed an ESE-WNW direction and only few of them showed an NNE-SSW direction. In addition, there are faults with opposite dip direction (synthetic and antithetic faults) and as result, highs and troughs were developed internally to the basin, during the sedimentation (Figure 6a). The above faults showed movements of the downthrown blocks ranging from 2 cm up to 30 cm. Finally, this tectonic activity seems to terminate in the upper stratigraphic outcropped level, during the sedimentation (light green line on Figure 6a,b).

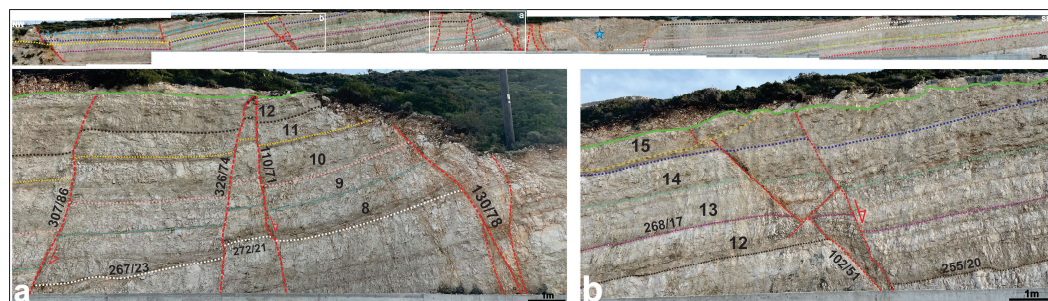


**Figure 6.** On the top and in the general view of the studied section the exact location of photographs a, b were marked with white boxes. (a,b) The activity of synthetic and antithetic normal faults with an ESE-WNW are marked. See the intrabasinal basement high or the synthetic scale with 2 cm up to 30 cm displacement. Light green line in the upper stratigraphic outcropped level shows the end of the tectonic activity during sedimentation.

### 5c. Giant slide

In western part of the studied section, a detachment surface, on which a giant slide was took place, up to 5 m thick, was recognized (yellow dashed line, in Figure 7a,b). This detachment surface crosscut the pre-existing faults, and moves the whole block to the west. The above slide indicates an instability of the basin floor with consolidated sediments producing a movement at least for 0.9 m to the west (Figure 7a,b).

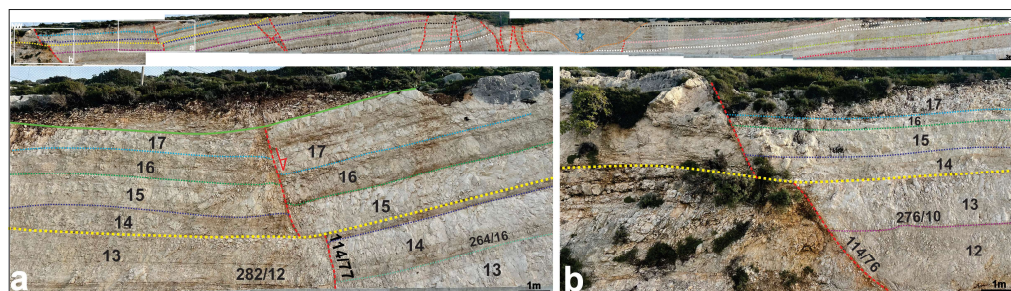


**Figure 7.** On the top and in the general view of the studied section the exact location of photographs **a, b** were marked with white boxes. **(a,b)** In two different locations, a detachment surface produced a huge block – giant slide (yellow line) up to 5m thick. The giant slide moved to the west for at least 0.9m.

### Additional data

Moreover, in the eastern side of the studied section recent fluvial deposits were recognized in a channelized geometry body that seems to follow a N-S direction, parallel with the major measured faults direction (Figure 8).



**Figure 8.** On the top and in the general view of the studied section the exact location of photograph is marked with white box. A channel geometry body, with N-S direction and erosional base, filled up with recent fluvial deposits showing that measured faults are still active.

It seems that the synchronous activity of synthetic and antithetic faults produced a subsided block, with a channel geometry, where the river was flowed (Figure 8) and eroded the underlying deposits. In the main channel axis, with more than 10m width, more than 4m thick deposits were accumulated. It is not clear if this event took place before or after the movement of the giant slide and if the same faults influenced the two different events. In now days this channel is situated 85m over sea level, without any clear evidence about the time of its development.

### 6. Discussion

The detailed analysis of the studied section and taking into account, our microfacies results from the surrounding areas, and the pre-existing previous results, different approaches for the sedimentary conditions, the basin evolution and the interaction between different factors, were arranged. These approaches referred to the depositional environments and the dynamic conditions of the carbonate sequence in the northern part of Paliki Peninsula, part of Kefalonia Island.

Microfacies analysis showed two different types of depositional conditions (FZ3/FZ4 and FZ7/FZ8). The samples from studied section showed that they were deposited either in deep-water conditions, in a pelagic environment (FZ3/FZ4), or in a shallower water condition, in an open marine-restricted environment (FZ7/FZ8). The deep-water samples that are situated close to the Atheras fault, in a very restricted but elongate basin, introducing that during Cretaceous the above fault plane acted as normal fault, with listric geometry, dips to the west and deep-water conditions were developed in its hangingwall block. From the other hand Enos fault plane dips to the east and gradually the basin was deepening eastwards towards the Ionian basin. Later and during the compressional regime (middle Miocene) Atheras faults inverted to back-thrust fault and Enos inverted to thrust fault. Moreover, the synchronous activity of Atheras and Enos fault created an intrabasinal high, in the block between them (Figure 9a, b).

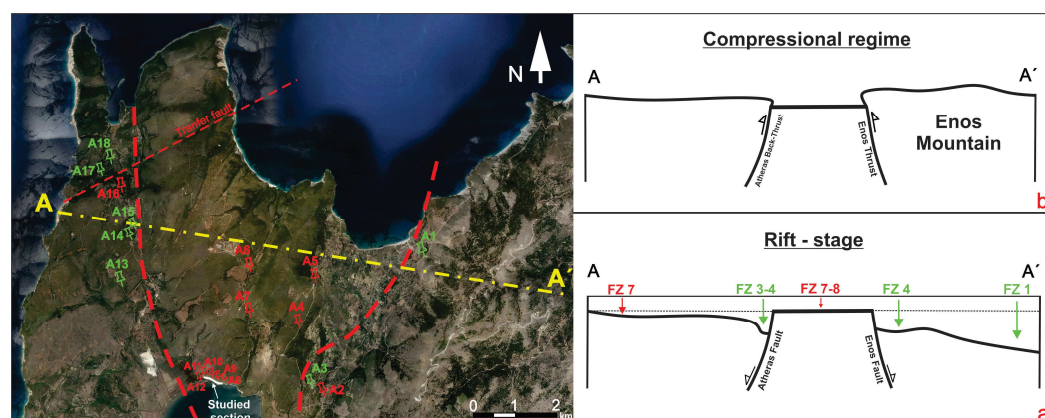


**Figure 9.** Modified from Google earth a map where the major faults (red dashed lines) were added, and the different depositional conditions of the studied samples are shown with different pin colors. The red pins show shallow water conditions and the green pins deep waters conditions according to microfacies analysis of the studied thin sections. Additionally, for a cross-section A-A', with a WNW-ESE direction, two proposed conditions, during the rift stage and during the compressional regime, were introduced.

As the studied area is situated far from Ionian thrust and taking into account present results in combination with the previous results [13,15,23] it seems that Apulian Platform was very close to west of the studied Paliki Peninsula.

It is obvious that the Enos fault, acting as a normal fault, during the Cretaceous, was the responsible fault due to the activity of the studied area was developed. Due to the activity of the above fault, the studied section rotated to the west and an unstable basin floor was formed, from which the giant slide was produced.

### 7. Conclusions

Three major points—events took place, with chronological order. First, two slumps were developed and sourced from the east and from the uplifted footwall of a normal fault situated east of the studied section. Second, many normal faults cross cut the studied sections, with listric geometry, displacement up to 30 cm, and with an ESE-WNW direction, mostly west dipping and less east dipping, producing either a synthetic scale or a horst geometry. These faults acted during the sedimentation as their activity ended before the end of the sedimentation. Third, a giant slide was produced, as a result of an unstable basin floor due to the whole block rotation to the west and the instability of the sediments. This slide cut the pre-existing normal faults and the block moved at least for 0.9 m to the west.

**Author Contributions:** Conceptualization N.D. and A.Z.; methodology, N.D., G.I. and A.Z.; software, N.D.; formal analysis, N.D., G.I., E.Z., P. P., and N.B.; investigation, N.D., G.I. and A.Z.; resources, N.D.; data curation, N.D.; writing—original draft preparation, N.D., G.I. and A.Z.; writing—review and editing N.D., G.I., N.B. and A.Z.; supervision, A.Z.; All authors have read and agreed to the published version of the manuscript.

**Acknowledgments:** Nicolina Bourli is a Post-Doc Researcher, and she was financially supported by the “Hellenic Hydrocarbon Resources Management S.A. (HHRM S.A.)”.

**Conflicts of Interest:** The authors declare no conflict of interest.

## References

1. Cooper MA, Williams GD, de Graciansky PC, Murphy RW, Needham T, De Paor D, Stoneley R, Todd SP, Turner JP, Ziegler PA (1989). Inversion tectonics -- a discussion. In *Inversion Tectonics*, Cooper, M.A., Williams, G.D. Eds.; Geological Society Special Publications: London 44:335-347.
2. Cooper M, Warren MJ (2020). Inverted fault systems and inversion tectonic settings. *Regional Geology and Tectonics: Principles of Geologic Analysis*, 169–204.
3. Williams GD, Powell CM, Cooper MA (1989). Geometry and kinematics of inversion tectonics. *Geological Society Special Publications*; London, 44:3-15.
4. Burbank DW, Leland J, Fielding EJ, Anderson RS, Brozovic N, Reid MR, Duncan C. (1996). Bedrock incision, rock uplift and threshold hillslopes in the northwestern Himalayas. *Nature* 379: 505–10. DOI:10.1038/379505a0.
5. Larsen IJ, Montgomery DR, Korup O. (2010). Landslide erosion controlled by hillslope material. *Nature Geoscience* 3(4): 247–51. DOI:10.1038/NGEO776.
6. Guzzetti F, Cardinali M, Reichenbach P. (1996). The influence of structural setting and lithology on landslide type and pattern. *Environmental & Engineering Geoscience* 2(4): 531–55. DOI:10.2113/gsegeosci.ii.4.531.
7. Scheingross JS, Minchew BM, Mackey BH, Simons M, Lamb MP, Hensley S. (2013). Fault-zone controls on the spatial distribution of slow-moving landslides. *Geological Society of America Bulletin* 125(3–4): 473–89. DOI:10.1130/B30719.1.
8. Densmore AL, Anderson RS, McAadoo BG, Ellis MA. (1997). Hillslope evolution by bedrock landslides. *Science* 275(5298): 369–72. DOI:10.1126/science.275.5298.369.
9. Chen A, Darbon J, Morel J-M. (2014). Landscape evolution models: A review of their fundamental equations. *Geomorphology* 219(C): 68–86. DOI:10.1016/j.geomorph.2014.04.037.
10. Bucci F., Santangelo M., Cardinali M., Fiorucci F., and Guzzetti F. (2016). Landslide distribution and size in response to Quaternary fault activity: the Peloritani Range, NE Sicily, Italy, *Earth Surf. Proc. Land.*, 41, 711–720, DOI: 10.1002/esp.3898.
11. Earle S. (2019). *Physical Geology – 2nd Edition*. Victoria, B.C.: BC campus: British Columbia, Canada; pp. 493-498.
12. Zelilidis, A., Piper, DJW., Vakalas, J., Avramidis, P., Getsos, K. (2003). Oil and gas plays in Albania: do equivalent plays exist in Greece? – *Journal of Petroleum Geology*, 26(1), 29-48.
13. Tserolas, P., Maravelis, A., Pasadakis, N., Zelilidis, A. (2018). Organic geochemical features of the Upper Miocene successions of Lefkas and Cephalonia islands, Ionian Sea, Greece: An integrated geochemical and statistical approach. *Arabian Journal of Geosciences*. doi.org/10.1007/s12517-018-3431-8.
14. Bourli N, Maravelis A.G, Zelilidis A (2020). Classification of soft sediment deformation in carbonates based on the Lower Cretaceous Vigla Formation, Kastos, Greece. *International Journal of Earth Sciences*, 109:2599–2614.
15. Accordi, G., Carbone, F., Di Carlo, M., Pignatti, J. (2014). Microfacies analysis of deep-water breccias clasts: A tool for interpreting shallow-vs. deep-ramp Paleogene sedimentation in Cephalonia and Zakynthos (Ionian Islands, Greece). *Facies*, 60, 445–466.
16. Accordi G., Carbone F., Pignatti J. (1999). Depositional history of a Paleogene carbonate ramp (western Cephalonia, Ionian Islands, Greece). *Geol Romana* 34(1998): 131–205.
17. Dunham RJ (1962). Classification of carbonate rocks according to depositional texture. In *Classification of Carbonate Rocks*, Ham, W.E., Ed; American Association of Petroleum Geologists, Tulsa, 108–121.
18. Embry AF, Klován JE (1971). A late Devonian reef tract on northeastern Banks Island. N.W.T. *Bulletin of Canadian Petroleum Geology*, 19:730–781.
19. Flügel E (2004). *Microfacies Analysis of Carbonate Rocks*. Springer Verlag, Berlin.
20. Hottinger L (1974). Alveolinids, Cretaceous-Tertiary larger Foraminifera. Exxon Production Research Company, Technical Information Services. Laboratories, 87:106.
21. Hottinger L (1997). Shallow benthic foraminiferal assemblages as signals for depth of their deposition and their limitations. *Bulletin de la Société Géologique de France* 168:491–505.
22. Pomoni-Papaioannou F, Zoumpouli E, Zelilidis A, Iliopoulos G (2012). Microfacies and benthic foraminiferal assemblages of the carbonate succession of the Cretaceous platform in the Sami area (NW of Kefallinia, W Greece): Biostratigraphy and palaeoenvironments. 29th IAS Meeting of Sedimentology. September 10-13, Schladming, Austria.
23. Bourli N, Kokkaliari M, Dimopoulos N, Iliopoulos I, Zoumpouli E, Iliopoulos G, Zelilidis A (2021). Comparison between siliceous concretions from the Ionian Basin and the Apulian Platform Margins (Pre-Apulian zone), western Greece: Implication of differential diagenesis on nodules evolution. *Minerals*, 11:890. <https://doi.org/10.3390/min11080890>